Fig. 2: A visual comparison of the performance of image enhancement and segmentation using enhanced and unenhanced data. (a) Example resulting enhanced images from the proposed enhancement-calibration deep learning model with selected high-quality data, compared to unenhanced data. (b) The predictive masks for slices in (a), trained with enhanced and unenhanced data, compared to the ground truth labels. Red circles indicate the missing or inaccurate portion when segmented using the unenhanced data.

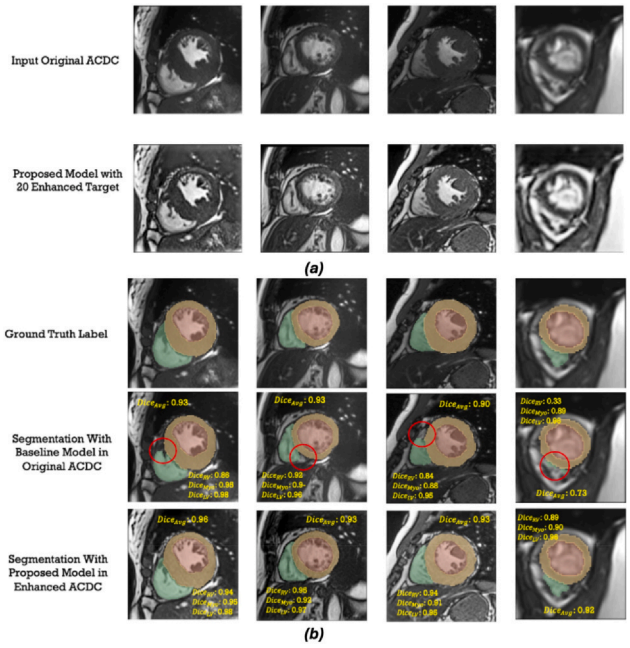

Fig. 3: Comparison of Segmentation Performance Metrics and Dice Score Distribution with Unenhanced and Enhanced ACDC. (a) Quantitative Analysis of Dice Score, ICC, and CoV for Segmentation with Unenhanced and Enhanced ACDC. (b) Statistical Distribution of Dice Scores for Segmentation using Baseline (Unenhanced) and Enhanced Data from the Proposed Model with 20 Enhanced Targets. All evaluations were averaged over five cross-validation folds. CoV: Coefficient of Variation, ICC: Intraclass Correlation.

Target in Enhancement	$Dice_{RV\_Endo}$	$Dice_{LV\_Myocardium}$	$Dice_{LV\_Endo}$	$Dice_{Avg}$
Proposed (Enhanced)	0.94	0.89	0.97	0.93
Baseline (Unenhanced)	0.90	0.86	0.96	0.91

	EDV_{RV_Endo}		$EDV_{LV\_Myocardium}$		EDV_{LV_Endo}	
	ICC	CV	ICC	CV	ICC	CV
Proposed (Enhanced)	0.95	3.98	0.92	3.52	0.99	1.68
Baseline (Unenhanced)	0.65	9.33	0.90	5.23	0.98	2.07

(a)

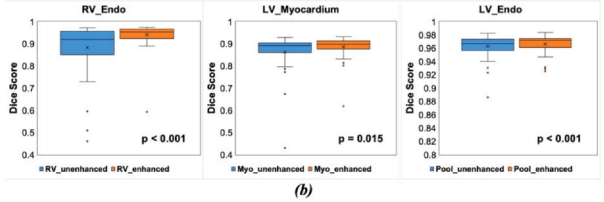

(b)

https://doi.org/10.1016/j.jocmr.2024.101491

Concealed deep phenotype abnormalities in subclinical hypertrophic cardiomyopathy detected by advanced imaging

George Joy, PhD[1], Michele Orini, PhD[2], Rhodri Davies, MD, PhD[3], Peter Kellman, PhD[4], Maite Tome, PhD[1], Pier Lambiase, MD, PhD[5], Erica Dall'Armellina, PhD[6], Gabriella Captur, MD, PhD[5], James C. Moon, MD[5], Luis Lopes, PhD[5]

[1] *St Georges University of London, London, United Kingdom*
[2] *Kings College London, London, United Kingdom*
[3] *Institute of Cardiovascular Sciences at University College London/Barts Heart Centre, London, United Kingdom*
[4] *National Heart Lung and Blood Institute, National Institutes of Health, Bethesda, MD*
[5] *University College London, London, United Kingdom*
[6] *University of Leeds, Leeds, United Kingdom*

Background: Predicting disease penetrance in individuals with pathogenic sarcomere mutation (G+) without hypertrophy (LVH-) is a significant clinical challenge in hypertrophic cardiomyopathy, that currently requires lifelong imaging surveillance. We combined deep phenotyping with machine learning to detect abnormalities that may be missed by conventional tests.

Methods: We performed a multicentre study on 155 individuals: 61 G+LVH- and 94 overt LVH+ (49 G+ / 45 G-). All participants underwent advanced CMR with diffusion tensor imaging, quantitative perfusion and electrocardiographic imaging.

Parameters employed in unsupervised machine learning included those reflecting LVH (maximum wall thickness [MWT] analyzed using AI algorithms), ischaemia (myocardial perfusion reserve [MPR]), microstructural alteration (fractional anisotropy [FA], sheetlet orientation [E2A]), epicardial conduction (mean activation time [mean AT], gradients [GATmean/max] and fractionation) and repolarization (mean activation recovery interval corrected [mean ARIc], range of ARIc, gradients GRTcmean/max).

We performed unsupervised machine learning using agglomerative hierarchical cluster analysis. Redundant CMR metrics were eliminated by removing features where pair-wise correlation was $r > 0.7$. The dissimilarity matrix was calculated using Euclidean distance and clusters were joined using Ward's method, which can separate clusters even in the presence of some noise. The optimal number of clusters was chosen using the NBclust library, which chooses the best consensus by evaluating multiple clustering validation indices. All clustering was performed blinded to clinical data (demographics, genotype, LVH thresholds, abnormal ECG).

Results: Cluster validity indices calculated using advanced phenotyping implied that there were three optimal clusters (Figure). Cluster 1 represented a mild deep phenotype (low MWT), with preserved microvascular function (higher MPR) and more preserved microstructure (higher FA, lower E2A). Repolarization was not prolonged (lower mean ARIc) but other EP changes were similar to cluster 2 (mean AT, GAT) and cluster 3 (Fractionation and GRTc).

Clusters 2 and 3 displayed intermediate and severe phenotypes respectively in terms of LVH (MWT higher than cluster 1 and less than 3), ischaemia (MPR was higher than cluster 1 and less than 3), and microstructural alteration (FA was lower than cluster 1 and higher than 3). EP changes were less severe in cluster 2 than cluster 3 in all parameters except for fractionation and GAT.

33% of subclinical HCM clustered in intermediate or severe deep phenotypes. These individuals had no difference in MWT and 50% had a normal ECG.

Conclusion: A high prevalence of subclinical HCM have an intermediate or severely abnormal deep microstructural, microvascular and EP phenotype. This subgroup had no LVH and normal 12-lead ECG, therefore are only detected by deep phenotyping techniques.

Figure. Heat map with dendrogram to show phenotypic clustering based on hypertrophy, microvascular function, microstructural alteration and ECG Imaging parameters. Each row represents a participant. (abbreviations as per Table)

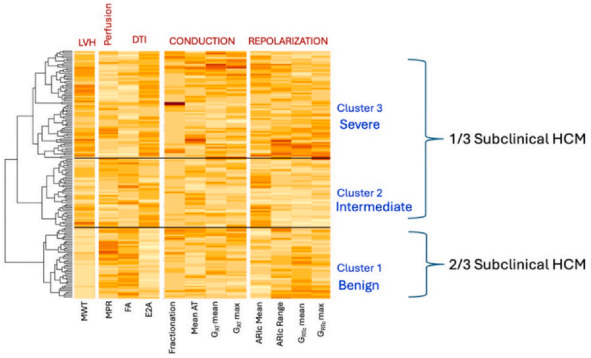

Phenotypic clustering based on hypertrophy, microvascular function, microstructural alteration and ECG Imaging parameters.

	Cluster 1 n = 44	Cluster 2 n = 43	Cluster 3 n = 68	P values 1vs2	2v3	1vs3
MWT	9.7(8.6-10.4)	15.7(11.7-17.2)	17.6(15.1-22.0)	< **0.001**	< **0.001**	< **0.001**
MPR	3.26(2.60-3.86)	2.77(2.31-3.25)	2.21(1.95-2.89)	**0.005**	**0.002**	< **0.001**
FA	0.32(0.31-0.33)	0.29(0.28-0.31)	0.28(0.25-0.29)	< **0.001**	< **0.001**	< **0.001**
E2A	45.2(42.3-49.8)	59.2(54.6-63.8)	62.9(57.3-65.5)	< **0.001**	0.056	< **0.001**
Mean AT	39(35-45)	31(36-44)	41(37-46)	0.53	0.16	**0.031**
Fractionation	12(2-36)	5(0-13)	13(1-36)	**0.013**	**0.008**	0.98
GATmean	0.41(0.33-0.50)	0.38(0.29-0.45)	0.43(0.33-0.57)	0.08	**0.006**	0.23
GATmax	4.8(4.4-5.5)	4.43(4.1-5.2)	5.6(4.6-6.6)	0.14	< **0.001**	**0.007**
Mean ARIc	241(226-254)	280(243-297)	272(253-293)	< **0.001**	0.89	< **0.001**
ARIc Range	188(178-205)	158(144-171)	201(183-218)	< **0.001**	< **0.001**	0.15
GRTcmean	1.2(1.1-1.4)	0.83(0.72-0.99)	1.1(1.0-1.3)	< **0.001**	< **0.001**	0.19
GRTcmax	11.4(10.1-13.3)	9.9(8.8-11.0)	12.4(10.4-14.5)	< **0.001**	< **0.001**	0.2

https://doi.org/10.1016/j.jocmr.2024.101492

Physics-informed deep learning model selection for robust segmentation of multi-center stress perfusion datasets: results from the SCMR registry

Dilek M. Yalcinkaya, MSc[1], Arian M. Sohi, BSc[2], Khalid Youssef, PhD[3], Luis F. Zamudio, MSc[4], Michael Elliott, MD[5], Venkateshwar Polsani, MD[6], Rohan Dharmakumar, PhD[7], Robert Judd, PhD[8], Matthew S. Tong, DO[9], Dipan J. Shah, MD[10], Orlando Simonetti, PhD[9], Behzad Sharif, PhD[1]

[1] *Purdue University, Indianapolis, IN*
[2] *Laboratory for Translational Imaging for Microcirculation, Weldon School of Biomedical Engineering, Purdue University, Indianapolis, IN*
[3] *Krannert Cardiovascular Research Center, Indianapolis, IN*
[4] *Indiana university, Hawthorne, CA*
[5] *Atrium Health Sanger Heart & Vascular Institute Kenilworth, Charlotte, NC*
[6] *Piedmont Healthcare, Piedmont Heart Institute, Atlanta, GA*
[7] *Indiana University School of Medicine, Indianapolis, IN*
[8] *Intelerad Medical Systems, Raleigh, NC*
[9] *The Ohio State University, Columbus, OH*
[10] *Weill Cornell Medical College, Houston Methodist DeBakey Heart and Vascular Center, Houston, TX*

Background: Accurate segmentation of stress first-pass perfusion (FPP) CMR is critical for reliable myocardial blood flow analysis. Automated artificial intelligence (AI) solutions are essential for overcoming the inefficiencies and inconsistencies inherent in manual contouring of stress/rest FPP studies [1,2]. Recent advances in deep neural network (DNN)-based segmentation of CMR datasets show that uncertainty-guided model selection improves generalization to external datasets [3,4]. In this work, we propose a new approach that combines state-of-the-art (SOTA) uncertainty-based DNN model selection with CMR physics-informed features to improve segmentation accuracy across multi-center stress FPP datasets.

Methods: The DNN models in this study were trained using a motion-corrected stress FPP internal dataset (n = 80 stress/rest studies) and tested on three external sites from the SCMR Registry [5]. As described in Fig 1, in the first step, we pre-select the top 10 models based on the lowest uncertainty scores. Next, we employ a physics-informed analysis to evaluate the quality of each segmentation result (Fig 1-A). Specifically, outliers are identified by analyzing the temporal behavior of myocardial pixel time-curves, by measuring deviations in the centroid of the area under the time curve (Fig 1-B). The final segmentation solution is selected based on the lowest outlier score. A total of 106 patients from 3 centers in the registry we included in the external test dataset as described in Fig 2-A. To evaluate the performance of the proposed hybrid physics-informed approach vs. the uncertainty-based SOTA technique, we focused on two common segmentation errors in FPP images that are difficult to detect with Dice score [6]: Type I error, where bloodpool is mistakenly included in the segmented myocardium; and, Type II error, where areas with minimal blood flow (e.g., epicardial fat) are erroneously included in the segmentation.

Results: The proposed hybrid model selection approach demonstrated significantly improved performance compared to the SOTA method. The prevalence of Type I errors was reduced from 20.3% to 4.0%, and Type II errors were reduced from 7.7% to 1.0% ($p < 0.001$ for both). The improvement was most notable in cases where the SOTA approach resulted in subtle, yet critical segmentation errors as